



## New monoterpenoids from the stigmas of *Crocus sativus*

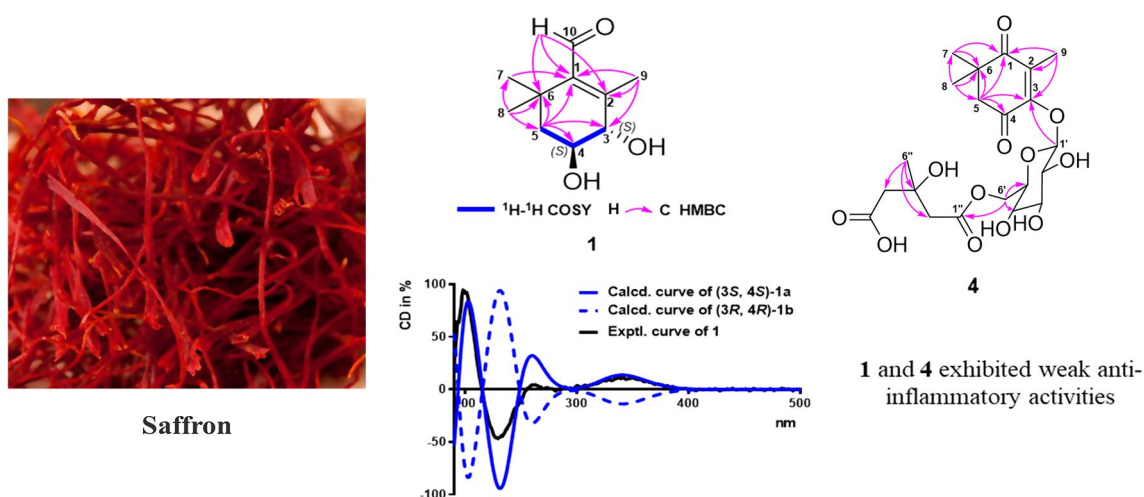
Qing-Wei Fang<sup>1</sup> · Wen-Wei Fu<sup>1</sup> · Jin-Ling Yang<sup>1</sup> · Yue Lu<sup>1</sup> · Jiang-Cheng Chen<sup>1</sup> · Pei-Ying Wu<sup>2</sup> · Xue Zhang<sup>2</sup> · Hong-Xi Xu<sup>1,3</sup>

Received: 19 April 2021 / Accepted: 10 August 2021  
© The Japanese Society of Pharmacognosy 2021

### Abstract

One new compound, crocusatin M (**1**), and three new glycosidic compounds, crocusatins N-P (**2–4**), along with nine known compounds were isolated from the dried stigmas of *Crocus sativus*. The structures of new compounds were elucidated on the basis of spectroscopic analysis, and the absolute configurations of **1**, **2**, and **3** were unambiguously assigned by the comparison of experimental and calculated ECD data. This is the first report of the isolation of **4** with the HMG moiety from the genus *Crocus*. Compounds **1** and **4** exhibited weak anti-inflammatory activities on inhibiting lipopolysaccharide (LPS)-induced NO production.

### Graphic abstract



**1** and **4** exhibited weak anti-inflammatory activities

**Keywords** *Crocus sativus* · Monoterpenoids · Structure elucidation · Anti-inflammation activity

Qing-Wei Fang and Wen-Wei Fu have contributed equally to this work.

✉ Wen-Wei Fu  
fu\_wenwei@163.com

✉ Hong-Xi Xu  
xuhongxi88@gmail.com

<sup>1</sup> School of Pharmacy, Shanghai University of Traditional Chinese Medicine, Cai Lun Lu 1200, Shanghai 201203, People's Republic of China

<sup>2</sup> Saffron Div. of Shanghai Traditional Chinese Medicine Co., Ltd, Shanghai 200002, People's Republic of China

<sup>3</sup> Shuguang Hospital, Shanghai University of Traditional Chinese Medicine, Shanghai 200002, People's Republic of China

## Introduction

*Crocus sativus* L. is a perennial herb that belongs to the Iridaceae family. It is an herb originating from the Middle East and can be cultivated around the world, e.g., in India, China, the Mediterranean basin, and Eastern Europe [1–3]. Saffron, the dried stigmas of *Crocus sativus* L., is an extensively used spice and food additive for its color and pleasant aroma, and it has also been widely used in folk medicine as an important phyto-therapeutic agent [4, 5] to treat mental disorders [6], neurodegenerative diseases [7], learning and memory dysfunctions [8], metabolic syndrome [9, 10], cardiovascular diseases [11], diabetes mellitus [10, 12], digestive disorders [13, 14], and cancers [14, 15]. Phytochemical investigations showed crocetin esters, picrocrocin and safranal are the major chemical constituents of saffron, and some of them showed a wide range of biological activities such as antiparasitic and antibacterial, antioxidant, hypotensive, cytotoxic, hypolipidemic, and diuretic activities [1, 3].

Inflammation is involved in many physiological and pathological processes of various disorders such as allergy, asthma, cardiovascular, and other related diseases [16]. Therefore, discovering new preventive and multi-potential agents for effective treatment of inflammatory conditions has been of great interest in recent years [17]. Previous studies showed that aqueous and ethanolic extracts of saffron have acute and/or chronic anti-inflammatory activity [18], saffron and its major chemical constituents can down-regulate pro-inflammatory cytokines, free radicals and the main molecules that participate in the pathogenesis of inflammatory based diseases [19, 20]. We recently reported the anti-inflammation activity of safranal on inhibiting macrophage-mediated inflammatory responses and alleviating DSS-induced colitis via inhibition of the MAPK and NF- $\kappa$ B signaling pathways [17].

In our search for novel biologically active compounds from natural sources, we were interested in the constituents of saffron due to its anti-inflammatory activity. In the present report, four new monoterpeneoids, crocusatins M-P (1–4), along with nine known compounds (5–13) (Fig. 1)

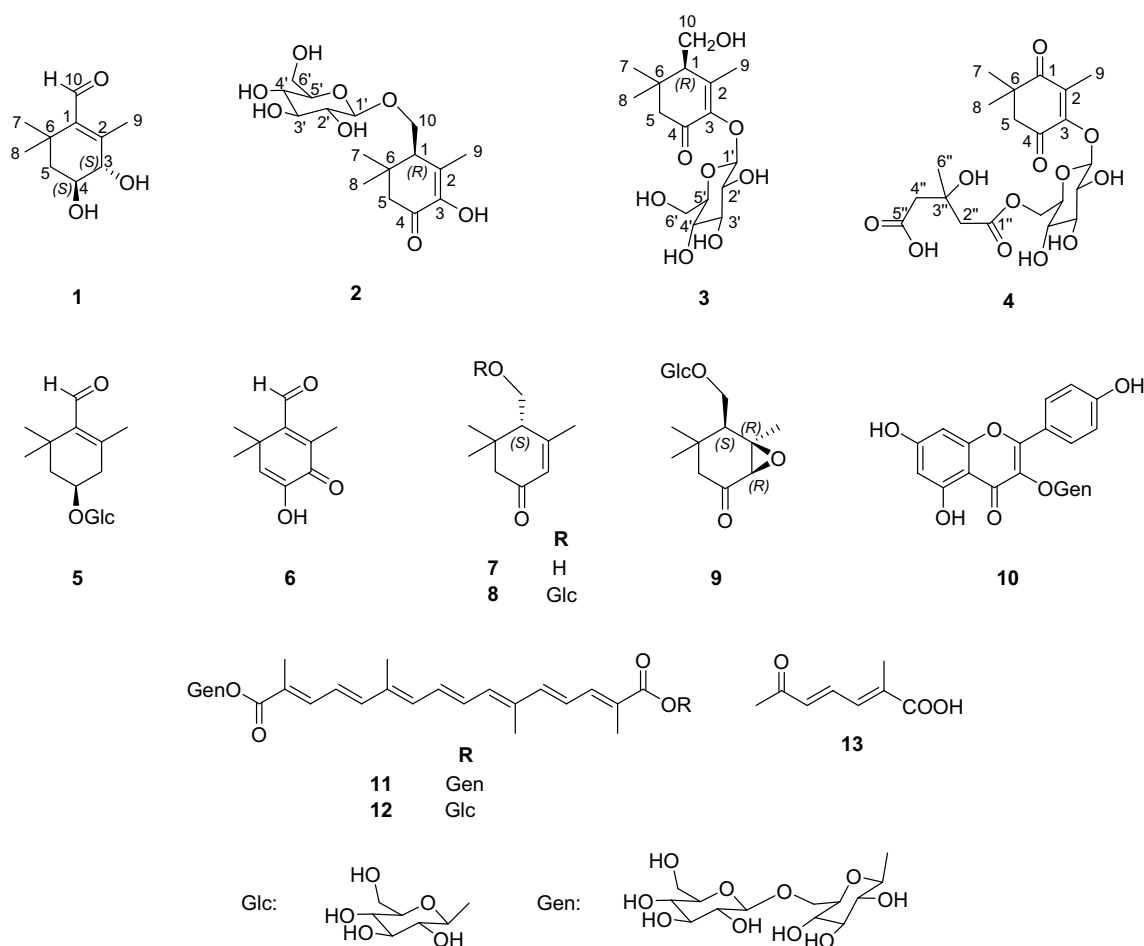


Fig. 1 Chemical structures of compounds 1–13

were isolated from the dried stigmas of *Crocus sativus*. Their structures were elucidated by HRESIMS, 1D and 2D NMR, and experimental and calculated electronic circular dichroism (ECD) data. The isolated compounds were evaluated for their anti-inflammatory activity on inhibiting lipopolysaccharide (LPS)-induced NO production in vitro.

## Results and discussion

The ethanolic extract of saffron was suspended in water and then partitioned with CH<sub>2</sub>Cl<sub>2</sub>. The H<sub>2</sub>O layer was subjected to a Diaion HP-20 column, followed by silica gel and reversed-phase C18 chromatography to afford one new monoterpene (**1**) and three new monoterpene glycosides (**2–4**), along with picrocrocin (**5**) [21], 4-hydroxy-2, 6, 6-trimethyl-3-oxocyclohexa-1,4-dienecarbaldehyde (**6**) [22], crocusatin C (**7**) [23], (4*S*)-4-hydroxy-3, 5,

5-trimethylcyclohex-2-enone 4-*O*- $\beta$ -D-glucopyranoside (**8**) [24], (1*R*, 5*S*, 6*R*)-5-(Hydroxymethyl)-4, 4, 6-trimethyl-7-oxabicyclo-[4.1.0] heptan-2-one *O*- $\beta$ -D-glucopyranoside (**9**) [21], kaempferol 3-*O*-(6-*O*- $\beta$ -D-glucopyranosyl)- $\beta$ -D-glucopyranoside (**10**) [25], crocin I (**11**) [24], crocin II (**12**) [24], and 6-oxo-2-methylhepta-2,4-dienoic acid (**13**) [26].

Compound **1** was isolated as an optically active, colorless oil. Its molecular formula was determined as C<sub>10</sub>H<sub>16</sub>O<sub>3</sub> based on the protonated molecular ion at *m/z* 185.1174 [M + H]<sup>+</sup> (calcd. 185.1178) in the HRESIMS spectrum. The <sup>1</sup>H NMR spectrum of **1** showed proton signals for an aldehyde at  $\delta_{\text{H}}$  10.11 (s, 1H), two oxygenated methines at  $\delta_{\text{H}}$  3.88 (dd, *J* = 8.1, 1.3 Hz, 1H) and 3.66 (m, 1H), a vinylic methyl at  $\delta_{\text{H}}$  2.20 (d, *J* = 1.1 Hz, 3H), a *gem*-dimethyls at  $\delta_{\text{H}}$  1.22 (s, 3H) and 1.28 (s, 3H), and one methylene at  $\delta_{\text{H}}$  1.66 (dd, *J* = 13.0, 3.8 Hz), and 1.54 (t, *J* = 12.6 Hz) (Table 1). The <sup>13</sup>C NMR and DEPT spectra indicated 10 resolved carbon signals, including a formyl at  $\delta_{\text{C}}$  193.3, two olefinic

**Table 1** <sup>1</sup>H and <sup>13</sup>C NMR data of compounds **1–4** in CD<sub>3</sub>OD<sup>a</sup>

No	<b>1</b>		<b>2</b>		<b>3</b>		<b>4</b>	
	$\delta_{\text{H}}$ ( <i>J</i> in Hz)	$\delta_{\text{C}}$						
1		140.2	2.47, t (4.2)	55.2	2.11, brs	55.7		204.3
2		154.8		158.6		150.9		133.9
3	3.88, dd (8.1, 1.3)	77.1		130.3		147.4		157.4
4	3.66, m	69.0		193.5		197.0		195.2
5a	1.54, t (12.6)	45.5	2.21, d (17.0)	49.8	2.10, d (17.4)	50.3	2.63, d (15.0)	52.4
5b	1.66, dd (13.0, 3.8)		2.94, d (17.0)		2.88, d (17.4)		2.91, d (15.0)	
6		35.1		35.7		35.6		46.7
7	2.20, d (1.1)	12.9	1.17, s	27.0	1.14, s	27.4	1.92, s	10.1
8	1.28, s	26.3	1.07, s	29.1	1.11, s	29.6	1.19, s	27.0
9	1.22, s	28.2	2.23, s	22.6	2.10, s	18.6	1.24, s	26.0
10a	10.11, s	193.3	3.87, dd (10.7, 4.2)	69.0	3.95, dd (11.9, 3.4)	61.5		
10b			4.25, dd (10.7, 4.2)		3.85, dd (11.9, 3.4)			
1'			4.22, d (7.8)	104.6	4.64, d (6.8)	104.5	5.40, d (7.3)	101.6
2'			3.13, dd (9.1, 7.8)	75.0	3.36, m	75.7	3.38, m	75.6
3'			3.32, m	78.3	3.36, m	78.1	3.42, m	77.7
4'			3.27, m	71.6	3.36, m	71.5	3.36, m	71.3
5'			3.27, m	78.1	3.20, m	78.3	3.38, m	75.9
6'a			3.67, m	62.8	3.67, dd (11.9, 5.2)	62.6	4.48, dd (12.0, 2.1)	64.0
6'b			3.88, m		3.79, dd (11.9, 2.4)		4.10, dd (12.0, 5.6)	
1''								172.2
2''a							2.71, d (14.5)	46.0
2''b							2.64, d (14.5)	
3''								70.7
4''							2.60, s	46.3
5''								174.9
6''							1.35, s	27.7

<sup>a</sup><sup>1</sup>H NMR data were measured at 400 MHz for **1** and **3**, and at 600 MHz for **2** and **4**, respectively; <sup>13</sup>C NMR data were measured at 100 MHz for **1** and **3**, and at 150 MHz for **2** and **4**, respectively. Proton coupling constants (*J*) in Hz are given in parentheses. The assignments were based on <sup>1</sup>H–<sup>1</sup>H COSY, HSQC, and HMBC experiments

quaternary carbons at  $\delta_C$  154.8 and 140.2, two oxygenated methines at  $\delta_C$  77.1 and 69.0, one methylene at  $\delta_C$  45.5, one saturated quaternary carbon at  $\delta_C$  35.1, and three methyls at  $\delta_C$  28.2, 26.3, and 12.9. The foregoing NMR evidences were similar to those of crocusatins J and K isolated from the same plant [27], indicating a congenetic 1,1,2,3-tetramethylcyclohexane-type monoterpene. The HMBC spectrum (Fig. 2a) displayed long-range  $^1\text{H}$ - $^{13}\text{C}$  correlations of Me-9/C-3, CH<sub>2</sub>-5/C-7, C-8 and C-4, indicating two hydroxyls were attached on C-3 and C-4. The planar structure of **1** was finally assigned through the detailed analysis of HMBC correlations.

The relative configuration at C-3 and C-4 was deduced from the coupling constant ( $J_{3,4} = 8.1$  Hz) based on the oxymethine proton singlet at  $\delta_H$  3.88 (dd,  $J = 8.1, 1.3$  Hz, 1H) in the  $^1\text{H}$  NMR spectrum of **1**, suggesting equatorial orientations of two hydroxyl groups at C-3 and C-4 [27]. Therefore, compound **1** had only one pair of enantiomers (**1a**: 3*S*,4*S* and **1b**: 3*R*,4*R*). The absolute configurations of **1** were assigned by comparison of the experimental and simulated electronic circular dichroism (ECD) spectra calculated using the time-dependent density functional theory (TDDFT). The overall calculated ECD spectra of **1a** was established based on the Boltzmann weighting of the lowest energy conformers, and the calculated ECD spectrum of **1a** was matched well with the experimental result (Fig. 2b). Based on the above evidence, the structure of **1** was determined to be as 3*S*, 4*S*-dihydroxy-2,6,6-trimethyl-1-cyclohexene-1-carboxaldehyde shown in Fig. 1 and was named crocusatin M.

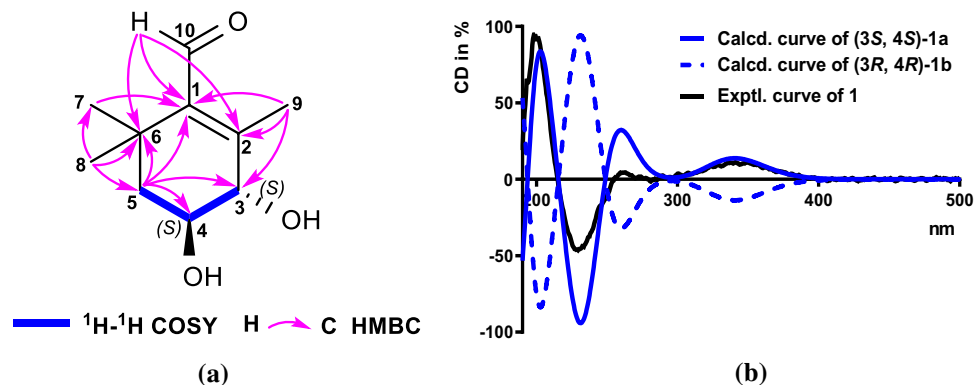
Compound **2** was obtained as a colorless solid. Its molecular formula was determined as C<sub>16</sub>H<sub>26</sub>O<sub>8</sub> by HRESIMS. The  $^1\text{H}$  NMR spectrum of **2** showed proton signals for one anomeric proton at  $\delta_H$  4.22 (d,  $J = 7.8$  Hz, 1H), two oxygenated methylenes at  $\delta_H$  4.25 (dd,  $J = 10.7, 4.2$  Hz, 1H) and 3.87 (dd,  $J = 10.7, 4.2$  Hz, 1H) and at  $\delta_H$  3.88 (m, 1H) and 3.67 (m, 1H), four oxygenated methines at  $\delta_H$  3.13, dd (dd,  $J = 9.1, 7.8$  Hz, 1H), 3.32 (m, 1H) and 3.27 (m, 2H), one methine proton signal at  $\delta_H$  2.47 (t,  $J = 4.2$  Hz, 1H), a vinylic methyl at  $\delta_H$  2.23 (s, 3H), and one *gem*-dimethyls

at  $\delta_H$  1.17 and 1.07 (s, 3H each) (Table 1). The  $^{13}\text{C}$  NMR and DEPT spectra of **2** displayed 16 carbon signals including a monoterpene moiety and one sugar moiety. The  $^1\text{H}$  and  $^{13}\text{C}$  NMR spectra of **2** were similar to those of 4-(hydroxymethyl)-3,5,5-trimethylcyclohex-2-enone- $\beta$ -D-glucoside [24] suggested that their structures were almost identical except that an olefinic proton signal lost in **2** and an olefinic carbon signal ( $\delta_C$  127.5) replaced by a downfield shifted carbon signal ( $\delta_C$  130.3) at C-3 in **2** indicating that another hydroxyl group was attached to C-3 in **2**, which was consistent with the additional oxygen atom in the molecular formula of **2**. Acid hydrolysis of **2** afforded D-glucose which was isolated and identified by comparison of the  $^1\text{H}$  NMR spectroscopic data and the specific rotation value with those of the authentic samples [D-glucose + 63.0 (c 0.10, H<sub>2</sub>O)]. The anomeric configuration of D-glucose was deduced as  $\beta$  by its anomeric proton coupling constant (Glc:  $J = 7.8$  Hz). The 2D structure of **2** was finally determined by the detailed COSY and HMBC spectra analysis. As shown in Fig. 3, the HMBC cross-peaks of H-1'/C-10 indicated the interlinkage between the sugar and monoterpene moiety.

There was only one chiral center (C-1) in the monoterpene moiety of **2**, which was determined by comparison of the experimental ECD spectrum of **2** and calculated ECD spectrum of the simplified structure of **2** (**2'R**, Fig. 3b and Figure CS4). Therefore, the structure of compound **2** was determined as 1*R*-(hydroxymethyl)-3-hydroxy-2, 6, 6-trimethyl-2-cyclohexen-4-one 10-O- $\beta$ -D-glucoside shown in Fig. 1 and designated as crocusatin N.

Crocusatin O (**3**) was obtained as colorless solid, and HRMS established its molecular formula as C<sub>16</sub>H<sub>26</sub>O<sub>8</sub>. The spectral data of **3** were similar to those of crocusatin N (**2**), and the  $^{13}\text{C}$  NMR data of **3** were superimposable on those of compound **2** except for the signals of C-2, C-3, and C-10. A downfield shifted carbon at  $\delta_C$  147.4 suggested that the interlinkage between sugar unit and monoterpene moiety was different from compound **2**. The structure of **3** was further confirmed by COSY and HMBC spectra. As shown in Fig. 3a, the HMBC cross-peaks of H-1'/C-3 indicated the interlinkage between the sugar and monoterpene

**Fig. 2** a The selected HMBC and  $^1\text{H}$ - $^1\text{H}$  COSY correlations of **1**; b experimental and calculated ECD spectra of **1**



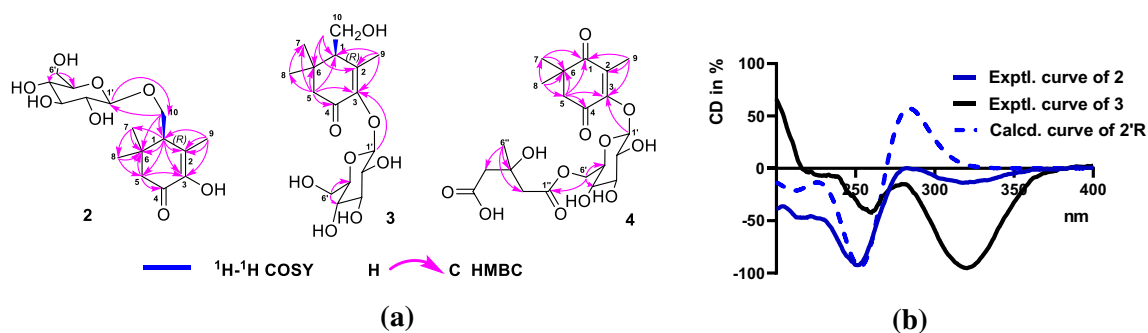


**Fig. 3** **a** Key NMR correlations of compounds **2**, **3**, and **4**; **b** experimental ECD spectra of **2**, **3** and calculated ECD spectrum of **2'R** (the aglycone of **2**)

moiety. The stereochemistry at C-1 was assigned as *R* by comparing the experimental ECD spectrum of **2** with that of **3** (Fig. 3b). Acid hydrolysis of **2** afforded D-glucose which was isolated and identified using the same method as described for **2**. Consequently, the structure of **3** was identified as 1*R*-(hydroxymethyl)-3-hydroxy-2, 6, 6-trimethyl-2-cyclohexen-4-one 2-*O*- $\beta$ -D-glucoside.

Crocusatins P (**4**) was also obtained as colorless solid, and HRMS established its molecular formula as  $\text{C}_{21}\text{H}_{29}\text{O}_{12}$ . The  $^1\text{H}$  and  $^{13}\text{C}$  NMR spectra of **4** (Table 1) in the aglycone part were very similar to those of **3** except for the presence of a carbonyl signal ( $\delta_{\text{C}}$  204.3) in **4** instead of the methanetriyl signals ( $\delta_{\text{H}}$  2.11, br s and  $\delta_{\text{C}}$  55.7) at C-1 in **3**. The structure of the aglycone part of **4** was further confirmed by COSY and HMBC spectra (Fig. 3a). In addition to the signals corresponding to the monoterpene moiety, the  $^1\text{H}$  and  $^{13}\text{C}$  NMR data of **4** obviously differed from those of **3** by the presence of a set of NMR signals corresponding to one 3-hydroxy-3-methylglutaryl (HMG) moiety which was confirmed by the detailed HMBC correlations analysis (Fig. 3a). Acid hydrolysis of **4** afforded sugar and the sugar was identified as D-glucose using the same method as described for **2** and **3**, and the  $\beta$ -anomeric configuration were deduced based on the coupling constant of the anomeric proton (Glc:  $J=7.3$  Hz). These results suggest that **4** is an HMG conjugate of monoterpene glycoside. The linkages between the HMG, sugar and monoterpene moieties were further confirmed by the HMBC correlations shown in Fig. 3a. Thus, the structure of **4** was finally established as 3-hydroxy-2, 6, 6-trimethylcyclohex-2-ene-1,4-dione 3-*O*-(3-hydroxy-3-methylglutaryl)- $\beta$ -D-glucopyranoside.

Compounds **1–4** were assessed for their anti-inflammatory effect on inhibiting lipopolysaccharide (LPS)-induced NO production in RAW264.7 macrophages and their cytotoxicity toward RAW264.7 cells. As shown in Table 2, compounds **1** and **4** exhibited weak inhibitory activity toward NO production with showing 29.47% and 30.08% inhibition at 1000  $\mu\text{M}$ , respectively. Compounds

**Table 2** Effects of compounds **1–4** on nitric oxide (NO) production in LPS-stimulated RAW264.7 cells and cytotoxicity toward RAW264.7 cells at 1000  $\mu\text{mol/L}$

Compounds	NO inhibition value (%)	Cell viability value (%)
<b>1</b>	29.47 $\pm$ 1.80	102.47 $\pm$ 6.18
<b>2</b>	23.12 $\pm$ 9.40	155.90 $\pm$ 7.24
<b>3</b>	13.74 $\pm$ 11.70	179.00 $\pm$ 17.23
<b>4</b>	30.08 $\pm$ 14.40	105.30 $\pm$ 9.99
Safranal <sup>a</sup>	83.76 $\pm$ 5.30 <sup>b</sup>	87.27 $\pm$ 2.50 <sup>b</sup>

<sup>a</sup>Positive control

<sup>b</sup>Assayed at 50.0  $\mu\text{M}$

**1–4** were not cytotoxic to RAW264.7 cells at 1000  $\mu\text{M}$ . Further, safranal used as a positive control was reassessed and exhibited inhibitory activity on NO production in RAW264.7 macrophages with an  $\text{IC}_{50}$  value of 19.69  $\mu\text{M}$ .

In conclusion, a new monoterpenoid (**1**), two new monoterpenoid glycosides (**2–3**), and a new monoterpenoid glycoside acylated with 3-hydroxy-3-methylglutaric acid (HMG-glycoside) (**4**), along with nine known compounds (**5–13**) were isolated from the dried stigmas of *Crocus sativus*. To the best of my knowledge, it is the first report of the isolation of monoterpenoid glycoside with the HMG moiety located at C-6 of glucose (**4**) from the family Iridaceae, which could be of value in the taxonomy of the genus *Crocus* or the family of Iridaceae. Compounds **1–4** were assessed for their anti-inflammatory effect in vitro, and compounds **1** and **4** exhibited weak inhibitory activity toward NO production without any cytotoxicity on the cell line. In the study, compounds **2–4** had the same sugar chain and a similar monoterpene aglycone, only compound **4** exhibited weak inhibitory activity on NO production, which suggested that the 3-hydroxy-3-methylglutaric acid (HMG) may be an important factor for potential anti-inflammatory activity in the monoterpenoid glycoside.

## Experimental

### General experimental procedures

The optical rotations and CD spectra were experimented by the Autopol<sup>®</sup> VI Automatic Polarimeter (Rudolph Research Analytical, Hackettstown, NJ, USA) and JASCO J-810 Circular Dichroism Spectropolarimeter (JASCO, Easton, MD, USA), respectively. The UV spectra was measured on Shimadzu UV-2700 UV-Visible Spectrophotometer (Shimadzu Corporation, Kyoto, Japan). The IR data were measured on VERTEX 70v FTIR Spectrometer (Bruker Optik GmbH., Ettlingen, Germany). The NMR spectra were recorded with Bruker Avance 400/600 NMR spectrometer (Bruker-Biospin, Billerica, MA, USA) and calibrated based on the solvent peak used. HRESIMS reports were obtained from a SYNAPT G2-Si HDMS (Waters Corp., Manchester, UK) with an electrospray ion source (Waters, Milford, MA) connected to a lock-mass apparatus that performed the real-time calibration correction. Analytical HPLC was performed on a Waters 2535 Series machine equipped with an Xbridge C<sub>18</sub> column (4.6×250 mm, 5 μm), and preparative HPLC was performed on a semi-preparative Xbridge Prep C<sub>18</sub> OBD column (19×250 mm, 5 μm). Column chromatography was performed on CHP20P MCI gel (75–150 μm, Mitsubishi Chemical Corporation, Japan), silica gel (200–300 mesh, Qingdao Haiyang Chemical Co., Ltd.), Sephadex LH-20 (GE Healthcare Bio-Sciences AB, Sweden), and reversed-phase C<sub>18</sub> silica gel (50 μm, YMC, Kyoto, Japan). Analytical and preparative TLC was performed on precoated GF254 plates (0.25 or 0.5 mm thickness, Qingdao Haiyang Chemical Co. Ltd.). Detection was performed by spraying the plates with 10% sulfuric acid followed by heating.

### Plant material

The saffron raw materials were collected at the Chongming Island in Shanghai city and were friendly donated by the Saffron Division of the Shanghai Traditional Chinese Medicine Co., LTD. (Shanghai, China) in August 2016. The scientific name was identified by one of the authors (Wenwei Fu). A voucher specimen (TCMNDD20160801) was deposited at the Engineering Research Centre of Shanghai Colleges for TCM New Drug Discovery (Shanghai University of Traditional Chinese Medicine).

### Extraction and isolation

Air-dried and powdered stigmas of the plant (930 g) were percolated successively with petroleum ether (20 L) and 80% EtOH (40 L) at room temperature. The combined

extracts were evaporated to dryness under vacuum to obtain a petroleum ether-soluble portion (fraction A, 34.6 g) and an 80% ethanol-soluble portion (320.7 g). Fraction A (33.0 g) was chromatographed on an MCI gel column, eluting with EtOH-H<sub>2</sub>O (0:100–95:5, v/v, successively) to yield seventeen fractions (Fr. A1-Fr. A17). Pale-yellow needle crystals (**6**, 128 mg) were obtained from Fr. A4.

Fraction B (300.0 g) was chromatographed on an MCI gel column, eluting with EtOH-H<sub>2</sub>O (0: 100 to 95:5, v/v, successively) to yield twenty-two fractions (Fr. B1-Fr. B22) based on the TLC profiles. Fr. B1 (180.0 g) was chromatographed on the MCI gel column again, and eluted in a step gradient of EtOH-H<sub>2</sub>O (0:100–95:5, v/v) to afford eight subfractions (Fr. B1a-B1h). Subfraction Fr. B1c was further separated on an MCI gel column using the same method as for Fr. B1 to give six subfractions (Fr. B1c1-Fr. B1c6), and Fr. B1c2 was purified by semi-preparative HPLC (MeCN-H<sub>2</sub>O, 5:95 → 30:70, 10 mL/min) to afford compounds **8** (15 mg), **3** (6 mg), and **9** (13 mg). Subfraction Fr. B1c5 was chromatographed on a Sephadex LH-20 column in MeOH and further purified by semi-preparative HPLC (MeCN-H<sub>2</sub>O, 5:95 → 30:70, 10 mL/min), yielding **2** (8.1 mg), **4** (4.1 mg), and **13** (18 mg). 15.1 mg of Fr. B2 was purified by semi-preparative HPLC (MeCN-H<sub>2</sub>O, 5:95 → 30:70, 10 mL/min) to give **1** (8.3 mg). 20.0 mg of Fr. B3 was purified by semi-preparative HPLC (MeCN-H<sub>2</sub>O, 5:95 → 30:70, 10 mL/min) to afford **7** (5.6 mg, *t<sub>R</sub>* = 17.6 min), and **10** (4.9 mg, *t<sub>R</sub>* = 14.0 min). 43 mg of Fr. B4 was purified by semi-preparative HPLC (MeCN-H<sub>2</sub>O, 20:80 → 80:20, 10 mL/min), yielding **11** (20.6 mg), and **12** (8.4 mg).

### Spectroscopic data (UV and IR, ms)

Crocusatin M (**1**): Colorless oil. <sup>1</sup>H NMR (CD<sub>3</sub>OD, 400 MHz) and <sup>13</sup>C NMR (CD<sub>3</sub>OD, 100 MHz) spectroscopic data, see Table 1; IR  $\nu_{\max}$  3321, 2928, 1672, 1063, 1019 cm<sup>-1</sup>; UV  $\lambda_{\max}$  (MeOH) (log  $\epsilon$ ): 216 (2.57), 246 (2.90) nm; HRESIMS *m/z* 185.1174 [M+H]<sup>+</sup> (calcd. for C<sub>10</sub>H<sub>17</sub>O<sub>3</sub>, 185.1178). [ $\alpha$ ]<sub>D</sub><sup>19.4</sup> +6.25 (*c* 0.096, MeOH); CD (MeOH) (log  $\Delta\epsilon$ ): 198 (+3.20), 230 (−2.89), 263 (+1.88), 281(−1.38), 341(+2.27) nm;

Crocusatin N (**2**): Colorless solid. <sup>1</sup>H NMR (CD<sub>3</sub>OD, 600 MHz) and <sup>13</sup>C NMR (CD<sub>3</sub>OD, 150 MHz) spectroscopic data, see Table 1; IR  $\nu_{\max}$  3344, 2911, 1672, 1608, 1020 cm<sup>-1</sup>; UV  $\lambda_{\max}$  (MeOH) (log  $\epsilon$ ): 215 (2.07), 252 (2.73) nm; HRESIMS *m/z* 345.1554 [M−H]<sup>−</sup> (calculated for C<sub>16</sub>H<sub>25</sub>O<sub>8</sub>); [ $\alpha$ ]<sub>D</sub><sup>19.7</sup> −37.26 (*c* 0.229, MeOH); CD (MeOH) (log  $\Delta\epsilon$ ): 190 (−3.18), 210 (+2.76), 253 (−2.87), 283 (+1.83) nm.

Crocusatin O (**3**): Colorless solid. <sup>1</sup>H NMR (CD<sub>3</sub>OD, 400 MHz) and <sup>13</sup>C NMR (CD<sub>3</sub>OD, 100 MHz) spectroscopic data, see Table 1; IR  $\nu_{\max}$  3340, 2467, 1657, 1590, 1375, 1070, 1034, 973 cm<sup>-1</sup>; UV  $\lambda_{\max}$  (MeOH) (log  $\epsilon$ ):

216 (1.84), 254 (2.45) nm; HRESIMS  $m/z$  345.1551  $[M-H]^-$  (calculated for  $C_{16}H_{25}O_8$ );  $[\alpha]_D^{20.2}$  -47.72 ( $c$  0.241, MeOH); CD (MeOH) (log  $\Delta\epsilon$ ): 192.5 (+2.57), 255.5 (-2.66), 283 (-1.05), 331 (-2.45), 481.5 (+1.64) nm.

Crocusatin P (**4**): Colorless solid.  $^1H$  NMR ( $CD_3OD$ , 600 MHz) and  $^{13}C$  NMR ( $CD_3OD$ , 150 MHz) spectroscopic data, see Table 1; IR  $\nu_{max}$  3382, 2931, 1698, 1671, 1617, 1376, 1066, 1019, 994  $cm^{-1}$ ; UV  $\lambda_{max}$  (MeOH) (log  $\epsilon$ ): 227 (2.06), 266 (2.68) nm; HRESIMS  $m/z$  473.1660  $[M-H]^-$  (calculated for  $C_{21}H_{29}O_{12}$ ).  $[\alpha]_D^{23.5}$  -17.02 ( $c$  0.235, MeOH).

### Sugar analysis

Compounds **2–4** (1.0–1.5 mg) were dissolved in 1 mol/L  $CF_3COOH$  (15 mL), and then the mixture was heated at 70 °C for 1 h [28]. The mixture was then extracted three times with EtOAc, and the aqueous layer was freeze-dried to obtain sugar (0.3–0.6 mg). By comparison of the  $^1H$  NMR spectroscopic data (Supplementary Information Figs. S46) and specific rotation with those of commercially available sugar samples, the sugar from the three compounds was identified as D-glucose  $[[\alpha]_D^{20} + 63.0$  to  $+316.7$  ( $c$  0.02–0.10,  $H_2O$ )].

### Anti-inflammatory evaluation in vitro by inhibiting lipopolysaccharide (LPS)-induced NO production

Measurement of cell viability: Cell viability was assessed via the MTT assay. RAW264.7 cells plated on 96-well plates ( $5 \times 10^4$  cells/well) were treated for 20 h with BDB. MTT (5 mg/mL) was subsequently added and incubated for 4 h. The culture medium was removed, and the cells were dissolved in 0.04 N HCl/isopropyl alcohol. The optical densities (OD) at 570 and 630 nm were measured with a microplate reader, and safranal (Sigma-Aldrich, purity  $\geq 90\%$ , stabilized) was used as a positive control.

Measurement of nitric oxide: RAW 264.7 cells ( $5 \times 10^5$  cells) were pre-incubated for 1 h with various concentrations of BDB and stimulated with LPS (200 ng/mL) at 37 °C for 24 h in medium. The culture supernatants were utilized to measure NO production. NO levels were determined by measuring nitrite levels in the culture media using Griess reagent (1% sulfanilamide, 0.1% N-1-naphthylethylenediamine dihydrochloride, and 2.5% phosphoric acid), and the absorbance was measured at 570 nm, and safranal was used as a positive control. Nitrite levels in the samples were calculated from a standard curve with known concentrations of sodium nitrite.

### Statistical analyses

All data were expressed as the mean  $\pm$  standard deviation (SD).

**Supplementary Information** The online version contains supplementary material available at <https://doi.org/10.1007/s11418-021-01559-1>.

**Acknowledgements** This work was financially sponsored partly by grants from the 3-year development plan project for Traditional Chinese Medicine (No. ZY (2018–2020)-CCCX-2001-02), Key-Area Research and Development Program of Guangdong Province (2020B1111110003), National Major Scientific and Technological Special Project for “Significant New Drugs Development” (2019ZX09301140), and NSFC (81803545 and 81973438). We also acknowledged the financial support partly from the Saffron Div. of the Shanghai Medicinal Material Co., Ltd.

### Declarations

**Conflict of interest** The funding sponsors had no role in the design of the study, in the collection, analyses, or interpretation of data, or in the decision to publish the results.

### References

- Ahrazem O, Rubio-Moraga A, Nebauer SG, Molina RV, Gomez-Gomez L (2015) Saffron: its phytochemistry, developmental processes, and biotechnological prospects. *J Agric Food Chem* 63:8751–8764
- Bukhari SI, Manzoor M, Dhar MK (2018) A comprehensive review of the pharmacological potential of *Crocus sativus* and its bioactive apocarotenoids. *Biomed Pharmacother* 98:733–745
- Mykhailenko O, Kovalyov V, Goryacha O, Ivanauskas L, Georgiyants V (2019) Biologically active compounds and pharmacological activities of species of the genus *Crocus*: a review. *Phytochemistry* 162:56–89
- Schmidt M, Betti G, Hensel A (2007) Saffron in phytotherapy: pharmacology and clinical uses. *Wien Med Wochenschr* 157:315–319
- Leone S, Recinella L, Chiavaroli A, Orlando G, Ferrante C, Leporini L, Brunetti L, Menghini L (2018) Phytotherapeutic use of the *Crocus sativus* L. (Saffron) and its potential applications: a brief overview. *Phytother Res* 32:2364–2375
- Shafiee M, Arekhi S, Omranzadeh A, Sahebkar A (2018) Saffron in the treatment of depression, anxiety and other mental disorders: current evidence and potential mechanisms of action. *J Affect Disord* 227:330–337
- Bian Y, Zhao C, Lee SM-Y (2020) Neuroprotective potency of saffron against neuropsychiatric diseases, neurodegenerative diseases, and other brain disorders: from bench to bedside. *Front Pharmacol* 11:579052. <https://doi.org/10.3389/fphar.2020.579052>
- Rajabian A, Hosseini A, Hosseini M, Sadeghnia HR (2019) A review of potential efficacy of saffron (*Crocus sativus* L.) in cognitive dysfunction and seizures. *Prev Nutr Food Sci* 24:363–372
- Razavi BM, Hosseinzadeh H (2017) Saffron: a promising natural medicine in the treatment of metabolic syndrome. *J Sci Food Agric* 97:1679–1685
- Giannoulaki P, Kotzakioulafi E, Chourdakis M, Hatzitolios A, Didangelos T (2020) Impact of *Crocus sativus* L. on metabolic profile in patients with diabetes mellitus or metabolic syndrome: a systematic review. *Nutrients*. <https://doi.org/10.3390/nu12051424>

11. Hatziagapiou K, Lambrou GI (2018) The protective role of *Crocus sativus* L. (Saffron) against ischemia-reperfusion injury, hyperlipidemia and atherosclerosis: nature opposing cardiovascular diseases. *Curr Cardiol Rev* 14:272–289
12. Moravej Aleali A, Amani R, Shahbazian H, Namjooyan F, Latifi SM, Cheraghian B (2019) The effect of hydroalcoholic Saffron (*Crocus sativus* L.) extract on fasting plasma glucose, HbA1c, lipid profile, liver, and renal function tests in patients with type 2 diabetes mellitus: a randomized double-blind clinical trial. *Phytother Res* 33:1648–1657
13. Khorasany AR, Hosseinzadeh H (2016) Therapeutic effects of saffron (*Crocus sativus* L.) in digestive disorders: a review. *Iran J Basic Med Sci* 19:455–469
14. Naeimi M, Shafiee M, Kermanshahi F, Khorasanchi Z, Khazaei M, Ryzhikov M, Avan A, Gorji N, Hassanian SM (2019) Saffron (*Crocus sativus*) in the treatment of gastrointestinal cancers: Current findings and potential mechanisms of action. *J Cell Biochem* 120:16330–16339
15. Khorasanchi Z, Shafiee M, Kermanshahi F, Khazaei M, Ryzhikov M, Parizadeh MR, Kermanshahi B, Ferns GA, Avan A, Hassanian SM (2018) *Crocus sativus* a natural food coloring and flavoring has potent anti-tumor properties. *Phytomedicine* 43:21–27
16. Medzhitov R (2008) Origin and physiological roles of inflammation. *Nature* 454:428–435
17. Lertnimitphun P, Jiang Y, Kim N, Fu W, Zheng C, Tan H, Zhou H, Zhang X, Pei W, Lu Y, Xu HX (2019) Safranal alleviates dextran sulfate sodium-induced colitis and suppresses macrophage-mediated inflammation. *Front Pharmacol* 10:1281
18. Hosseinzadeh H, Younesi HM (2002) Antinociceptive and anti-inflammatory effects of *Crocus sativus* L. stigma and petal extracts in mice. *BMC Pharmacol*. <https://doi.org/10.1186/1471-2210-2-7>
19. Boskabady MH, Farkhondeh T (2016) Antiinflammatory, antioxidant, and immunomodulatory effects of *Crocus sativus* L. and its main constituents. *Phytother Res* 30:1072–1094
20. Poursamimi J, Shariati-Sarabi Z, Tavakkol-Afshari J, Mohajeri SA, Mohammadi M (2020) *Crocus sativus* (Saffron): an immunoregulatory factor in the autoimmune and non-autoimmune diseases. *Iran J Allergy Asthma Immunol* 19(S1):27–42. [https://doi.org/10.18502/ijaai.v19i\(s1.r1\).2852](https://doi.org/10.18502/ijaai.v19i(s1.r1).2852)
21. Straubinger M, Bau B, Eckstein S, Fink M, Winterhalter P (1998) Identification of novel glycosidic aroma precursors in saffron (*Crocus sativus* L.). *J Agric Food Chem* 46:3238–3243
22. Zarghami NS, Heinz DE (1971) Monoterpene aldehydes and isophorone-related compounds of saffron. *Phytochemistry* 10:2755–2761
23. Li CY, Wu TS (2002) Constituents of the pollen of *Crocus sativus* L. and their tyrosinase inhibitory activity. *Chem Pharm Bull (Tokyo)* 50:1305–1309
24. Straubinger M, Jezussek M, Waibel R, Winterhalter P (1997) Novel glycosidic constituents from saffron. *J Agric Food Chem* 45:1678–1681
25. Tanaka M, Fujimori T, Uchida I, Yamaguchi S, Takeda K (2001) A malonylated anthocyanin and flavonols in blue *Meconopsis* flowers. *Phytochemistry* 56:373–376
26. Gao HY, Wang HY, Li GY, Du XW, Zhang XT, Han Y, Huang J, Li X, Wang JH (2014) Constituents from Zhuyeqing Liquor and their inhibitory effects on nitric oxide production. *Phytochem Lett* 7:150–155
27. Li CY, Lee EJ, Wu TS (2004) Antityrosinase principles and constituents of the petals of *Crocus sativus*. *J Nat Prod* 67:437–440
28. Zhang X, Han B, Feng Z, Jiang J, Yang Y, Zhang P (2018) Bioactive thionic compounds and aromatic glycosides from *Ligusticum chuanxiong*. *Acta Pharm Sin B* 8:818–824

**Publisher's Note** Springer Nature remains neutral with regard to jurisdictional claims in published maps and institutional affiliations.